Synergetic Effect of Sodium Citrate and Starch in the Synthesis of Silver Nanoparticles

Rita Kakkar,[1] E. D. Sherly,[1] Kalpana Madgula,[1] D. Keerthi Devi,[2] B. Sreedhar[2]

[1]*Department of Chemistry, St. Francis College for Women, Begumpet, Hyderabad 500016, India*
[2]*Inorganic and Physical Chemistry Division, Indian Institute of Chemical Technology (Council of Scientific and Industrial Research), Hyderabad 500607, India*

Received 25 July 2011; accepted 22 December 2011
DOI 10.1002/app.36727
Published online in Wiley Online Library (wileyonlinelibrary.com).

ABSTRACT: Silver nanoparticles (AgNPs) were prepared under mild conditions by exploiting a combination of naturally abundant polymer starch and trisodium citrate as reducing agent and stabilizing agent. Optimization of the concentration of starch, citrate, pH, and reaction time showed significant influence on the size of the NPs. The obtained NPs were well characterized by UV–Vis, transmission electron microscopy, X-ray diffraction, X-ray photoelectron spectroscopy, and thermogravimetric analysis. The effect of varying proportions of citrate and starch and the order of their addition to the reaction mixture with respect to their role as reducing or, and stabilizing agents was also studied. The antibacterial activity of thus prepared NPs is being reported. © 2012 Wiley Periodicals, Inc. J Appl Polym Sci 000: 000–000, 2012

Key words: silver; starch; sodium citrate; antibacterial; nanoparticles; stabilizing agent

INTRODUCTION

Noble metal nanoparticles (NPs) are envisaged to provide solutions to optical, electronic, biotechnological and environmental challenges in the areas of solar energy conversion, catalysis, medicine, and water treatment.[1] Size, shape, and surface morphology play pivotal roles in controlling the physical, chemical, optical, and electronic properties of these nanoscopic materials.[2] When compared with their macroscaled counterparts, they often show unique and considerably changed physical, chemical, and biological properties.[3] It is also an established fact that the size, morphology, stability, and properties of the metal NPs are strongly influenced by the experimental conditions, the kinetics of interaction of metal ions with reducing agents, and adsorption processes of stabilizing agent with metal NPs.[4,5] Thus, the synthesis of noble metal NPs for various novel applications has become a major field of research interest.[6]

Colloidal silver is of particular interest because of distinctive properties, such as, catalytic, antibacterial activity, good conductivity, and chemical stability.[7–9] Chemical reduction by the colloidal route is the most frequently applied method for the preparation of silver nanoparticles (AgNPs) as stable colloidal dispersions in water or organic solvents[10,11] and also via microemulsion,[12] polymer protection methods,[13–15] carbon nanotube,[16] and coprecipitation.[17,18] For producing well dispersed NPs, not only different organic molecules are used as templates but macromolecules in the form of block copolymers, liquid crystals,[19] biological macromolecules,[20,21] latex particles,[22] Dendrimers,[23–25] microgels, and hydrogels[26–28] are also used. Commonly used reductants are borohydride, ascorbate, hydrazine, and elemental hydrogen.[29–37]

This work emphasis majorly on some of the key issues like utilization of nontoxic chemicals, choice of the solvent medium used for the synthesis, environmentally benign reducing agent, and the choice of a nontoxic material for the stabilization of the NPs. Most of the synthetic methods reported to date rely heavily on organic solvents. This is mainly due to the hydrophobicity of the capping agents used.[38]

Previous studies showed that use of a strong reductant such as borohydride, resulted in small particles that were somewhat monodisperse, but the generation of larger particles was difficult to control.[39,40] Use of a weaker reductant such as citrate, resulted in a slower reduction rate, but the size distribution was far from narrow.[10,11,41] The high surface energy of these particles makes them extremely reactive, and most systems undergo aggregation without protection or passivation of their surfaces.[42–46] Some of the commonly used methods for surface passivation include protection by self-assembled monolayers, the most popular being citrate[47] and thiol-functionalized organics,[48] encapsulation in the H_2O pools of

Correspondence to: B. Sreedhar (sreedharbojja@gmail.com).

reverse microemulsions,[49] and dispersion in polymeric matrixes.[50] There are also references of reduction and stabilization of metal NPs by natural polymers like starch[38,51] and gum acacia.[52,53]

Among natural polymers, the use of starch is reported in many applications as it is one of the most promising biocompatible and biodegradable materials that is universally available and of low cost. Starch is a linear polymer (polysaccharide) made up of repeating glucose units linked by glucosidic linkages in the 1–4 carbon positions. There are two major molecules in starch: 10–30% amylose and 70–90% amylopectin[54] Amylose has α(1,4) links and one reducing end, and on the other hand amylopectin has α(1,6) branches in every 12–30 residues.

In this work, a combination of reduction and stabilization by citrate and starch together has been worked out. The method is efficient for the synthesis of well formed nanosilver crystalline particles stabilized by starch. The size and shape of the NPs produced can be controlled by varying the concentration of citrate, starch, temperature, pH, and reaction time. The resulting nearly monodispersed AgNPs are well characterized by UV–Vis, transmission electron microscopy (TEM), X-ray diffraction (XRD), X-ray photoelectron spectroscopy (XPS), and thermogravimetric analysis (TGA) techniques.

EXPERIMENTAL

Materials

$AgNO_3$ (analytical-reagent-grade) was purchased from SD Fine-Chem, Mumbai, and trisodium citrate dihydrate (analytical-reagent-grade) was purchased from Finar Chemicals, Ahmedabad, India, and starch was purchased from Merck, Mumbai. Double distilled water was used for the preparation of $AgNO_3$ and trisodium citrate solutions.

Preparation of the AgNPs

AgNPs were prepared by heating a solution of $AgNO_3$ with starch under reflux condition with a magnetic stirrer (Spinot Model MC − 02) for 15 min and followed by the addition of equal volume of sodium citrate (Na citrate) solution and stirring continued for 1 h at 95°C. The first sets of experiments were done by keeping the concentrations of $AgNO_3$ and Na citrate solution constant and varying the amounts of starch to find the optimum concentration of starch.

Similar sets of experiments were performed to study the effect of change in reaction time, temperature, concentration of sodium citrate, and pH of the solution and also the effect of changing the order in which starch and citrate are added.

Characterization

TEM samples were prepared by placing sample mixture drops directly on the Formvar polymer coated grids using micropipette. The AgNPs present in the aqueous mixture were allowed to settle, and the extra solvent was subsequently removed by placing TEM grid on a neat filter paper and dried at ambient temperature condition for half a day. The morphology, size, and shape distribution of the AgNPs were recorded using TECNAI FE12 TEM instrument operating at 120 kV. In each image, more than 150 particles were analyzed using SIS imaging software to create size distribution histogram. The diffraction patterns were recorded at selected area to determine the crystal structure and phases of crystals at 660 mm camera length.

All UV–Vis spectrophotometric characterization of aqueous dispersions were carried out on Perkin Elmer Lambda 750 spectrophotometer using quartz cuvette cells of 1 cm path length. Colloid samples were usually diluted with water by a factor of 5 or more if necessary and examined over the 900–190 nm region using a scan rate of 60 nm/min. XRD measurements of the AgNPs were recorded using a Rigaku diffractometer (Cu radiation, $\lambda = 0.1546$ nm) running at 40 kV and 40 mA (Tokyo, Japan). TGA was carried out on a TGA/SDTA Mettler Toledo 851^e system using open alumina crucibles containing samples weighing about 8–10 mg with a linear heating rate of $10°C\ min^{-1}$. Nitrogen was used as purge gas for all these measurements. XPS measurements were obtained on a KRATOS-AXIS 165 instrument equipped with dual aluminum–magnesium anodes using Mg K radiation ($h\nu = 1253.6$ eV) operated at 5 kV and 15 mA with pass energy 80 eV and an increment of 0.1 eV. The samples were degassed out for several hours in XPS chamber to minimize air contamination to sample surface. To overcome the charging problem, a charge neutralizer of 2 eV was applied and the binding energy of C 1s core level (BE = 284.6 eV) of adventitious hydrocarbon was used as a standard. The XPS spectra were fitted using a nonlinear square method with the convolution of Lorentzian and Gaussian functions after a polynomial background was subtracted from the raw spectra.

Antimicrobial activity

To examine the antibacterial effect of synthesized AgNPs, three different samples were made – AgNPs synthesized using starch, trisodium citrate, and starch in combination with trisodium citrate, loaded on a nutrient agar media. The agar medium was prepared by mixing 0.5 g of peptone, 3.0 g of beef extract, and 5.0 g of sodium chloride (NaCl) in 1000 mL distilled water, and the pH was adjusted to 7.0. Lastly,

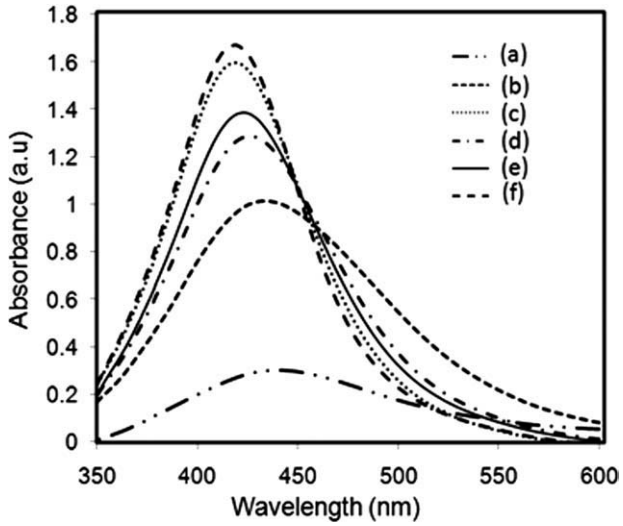

Figure 1 UV–Vis spectra for silver nanoparticles stabilized starch–citrate mixtures (a) no starch, (b) 0.0007*M*, (c) 0.0029*M*, (d) 0.0044*M*, (e) 0.0058*M*, and (f) 0.0090*M*.

15.0 g of agar was added to the solution. The agar medium was sterilized in a conical flask at a pressure of 15 lbs for 30 min. This agar was transferred into sterilized Petri dishes in a laminar air flow. After solidification of the media, Gram positive and Gram negative cultures were streaked on the solid surface of the media. To this inoculated Petri dish, one drop (75 μL) of synthesized AgNPs solutions (20 mg/10 mL distilled water) was added using 50 μL tip into the wells bored on the agar plate, and plates were incubated for 48 h at 37°C.

RESULTS AND DISCUSSION

Effects of changing starch concentration

To determine the reduction efficacy of Ag^+, a set of experiments were carried out by taking 0.001*M* $AgNO_3$, 0.01*M* Na citrate and by varying the concentration of starch (0.0007–0.009*M*) at 95°C for 1 h, and their respective UV–Vis spectra are presented in Figure 1. A band shift in the UV–visible spectra dependent on the particle size, chemical surrounding, adsorbed species on the surface, and dielectric constant, etc. is a unique characteristic of NPs.[46] Significant information drawn from the UV–Vis results illustrates that with an increase in starch concentration, there is a considerable improvement in the reduction efficacy as a monotonic increase of intensity with a blue shift of the peak maximum from 444 nm to 419 nm is observed as illustrated in Figure 2, and that can be attributed to a decrease of the average particle sizes. So, an optimum concentration of 0.003*M* starch has been selected for the rest of the work.

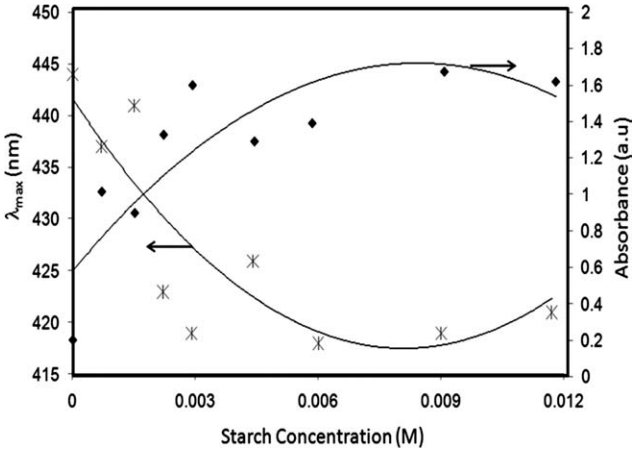

Figure 2 Variation of absorbance and λ_{max} with varying starch concentration between 0.0007*M* and 0.009*M*.

Effect of temperature and reaction time

To optimize the reaction temperature and time, two reactions were carried out. First, a reaction mixture with 0.001*M* $AgNO_3$, 0.01*M* Na citrate, and 0.003*M* starch kept at room temperature even for 2 days showed no change in color. On the other hand, when the reaction mixture was heated at 95°C and the progress of reaction monitored, the color of the solution changed from colorless to brown over 9 h course of the reaction. The reduction starts during the initial stages of the reaction, and NPs formation can be observed after 30 min. As the time progresses, the intensity of the surface plasmon absorption at 420 nm increases in intensity from 1.586 to 1.768 (9 h) as shown in Table I. A slight but steady blue shift of the peak from 420 nm to 412 nm is observed. This confirms that the reduction potentiality increases with time. The optimum time was fixed at 3 h at a reaction temperature of 95°C for further experiments.

Study of effect of sodium citrate concentration

To know the effect of the concentration of citrate on the size and concentration of the nanosilver particles produced, reactions were conducted with 0.001*M* $AgNO_3$, 0.003*M* starch at a temperature of 95°C with different concentrations of Na citrate. Increasing the

TABLE I
Variation of Absorbance and λ_{max} with Varying Reaction Times

Sample	Time (h)	λ_{max} (nm)	Absorbance (a.u)
A_2	1	420	1.586
B_2	2	415	1.610
C_2	3	412.7	1.630
D_2	4	413.2	1.640
E_2	5	413.2	1.706
F_2	9	412.7	1.768

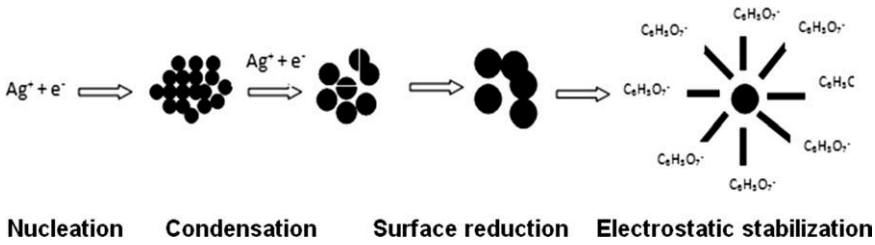

Figure 3 Reduction and stabilizatin of silver nanoparticles by sodium citrate.

trisodium citrate concentration from 0.001*M* to 0.03*M* keeping all other parameters same, no significant change in the absorption peak maximum (413 nm) is observed. So, to minimize the concentration of sodium citrate used in this study, all further experiments were carried at 0.002*M*. From all the initial experiments, the optimized reaction conditions for further studies were 0.001*M* $AgNO_3$, 0.003*M* starch, and 0.002*M* trisodium citrate at 95°C for 3 h.

Role of starch and citrate

Starch alone acts as both reducing and stabilizing agent when the reaction is carried out at elevated temperatures (~95°C). At this temperature, it is believed that starch can undergo hydrolysis and may give rise to free D-glucose units which have terminal aldehyde groups and are reducing in nature and thus contributing for the reduction of Ag^+ to nanosilver and further stabilizing the nanosilver formed. Well formed crystals of nanosilver are also obtained on reduction with citrate alone. The reduction of silver ions (Ag^+) in aqueous solution initially, leads to the formation of silver atoms (Ag^0), which is followed by agglomeration into oligomeric clusters. These clusters eventually lead to formation of colloidal Ag particles.[55] The stabilization of NPs in this case is due to the Helmholtz type double layer of charges of silver and citrate ions as shown in Figure 3.

Though nanosilver can be formed by the reduction of Ag^+ ions either by starch or citrate ion, yet we have used a combination of citrate and starch in this study as it gives much higher concentration of nanosilver particles with smaller size as can be seen from the increase in intensity of the surface plasmon peak and the blue shift. It appears that reduction by citrate predominates in our set up because when the reaction mixture is initially heated with starch, before addition of citrate no significant formation of nanosilver is seen even after heating for about half an hour under the experimental conditions, whereas when heating is done without starch using citrate alone nanosilver is formed within 5 min as can be seen in Figure 1(a). This is explained by the fact that in neutral solutions there is very minimal breakdown of starch to give reducing monomers units. Starch is thus primarily being used as a lyophilic stabilizer to cap up the AgNPs formed in this work.

Order of addition of starch and sodium citrate

Another trend that was noticed during this work is the order in which starch and sodium citrate was added. Addition of starch first and then citrate as mentioned in the procedure gave NPs with a very small size variation as indicated by narrow peak in the UV–visible spectra [Fig. 4(a)]. On reversing the order of addition, there appears to be a much broader distribution of particle size [Fig. 4(b)]. This may be due to the starch-controlled nucleation of AgNPs and the effective passivation of the surfaces and suppression of the growth resulting narrow size distribution through strong interactions with the particles via the functional molecular groups of starch.

Effect of pH

All the work reported till now is at pH 7. To study the effect of pH, reactions were carried out at pH 2, 7, and 10. On decreasing the pH from pH 7 to pH 2 with HNO_3, nanosilver formation is not observed. On the other hand, at pH 10, a peak at 413 nm with an absorbance of 1.939 was observed and is tabulated in Table II. This is explained by the fact that Ag+ ion exists as different species depending on the medium/pH of the solution. In aqueous silver nitrate, the Ag^+ ions exist in a hydrated form as $[Ag(H_2O)_2]^+$

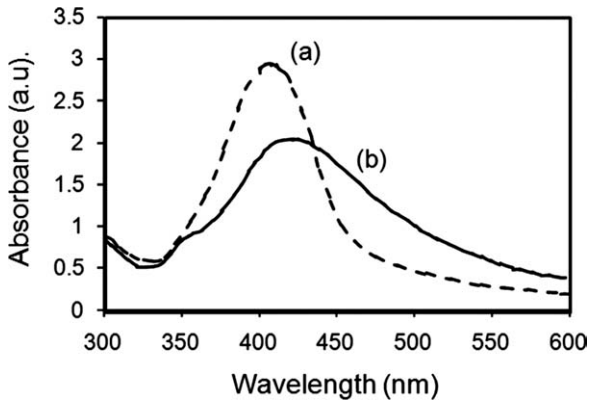

Figure 4 Role of addition of starch and citrate (a) starch first and citrate later and (b) citrate first and then starch.

TABLE II
Effect of pH and Sodium Citrate on the Formation of Silver Nanoparticles Stabilized with Starch

Sample	pH	Na citrate	λ_{max} (nm)	Absorbance
Reduction with starch and citrate	10	0.002*M*	413	1.939
Reduction with starch and citrate	7	0.002*M*	413	1.630
Reduction with starch and citrate	2	0.002*M*	No nanosilver formed	
Reduction with starch only	10	Nil	419	1.364
Reduction with starch only	7	Nil	417	0.221
Reduction with starch only	2	Nil	No nanosilver formation	

complex , whereas in the presence of NaOH, it is present as unstable $[Ag(OH)_2]^-$ ions which quickly dehydrates further to give silver oxide, Ag_2O precipitate. In ammonical solution, silver ions exists as $[Ag(NH_3)_2]^+$ complex in the mixture as in Tollens' reagent. Of the three complex species, $[Ag(NH_3)_2]^+$ present in ammonical medium is more easily reduced followed by $[Ag(H_2O)_2]^+$ present in neutral medium. Thus, nanosilver formation is more in ammonical medium followed by neutral and not formed at all in acidic medium with the weak reducing agents used here. This has been further confirmed by direct reaction of highly reducing dextrose and silver nitrate in acidic medium, where there is no nanosilver formation with or without the presence of sodium citrate.

Surprisingly, it was further noticed that even with starch alone at pH 10, reduction of Ag ions was readily taking place with an absorption peak at 419 nm though in lesser concentration as is observed from the absorbance values. Starch by itself is not a reducing agent, but it can be hydrolyzed to different extents by boiling in acid, neutral, or alkaline media. Hydrolysis to give reducing monosaccharides is maximum in the presence of mineral acids, H_2SO_4, and HCl, lesser in the presence of NH_4OH, and least in neutral medium. Yet, nanosilver is most effectively formed in the ammonical medium due to most easily reducible species $[Ag(NH_3)_2]^+$.

In all the UV–Vis spectra, the absence of the peak at 560 nm confirms no agglomeration of AgNPs or Ag cluster formation,[56] in other words, the NPs that form in this reaction are highly dispersed in nature. Remarkable stability (no aggregation) of the NPs was noticed in this investigation even after 5 months at room temperature.

TEM studies

To access the size and morphology of the AgNPs, we performed TEM and the images are presented in Figure 5. As can be seen from Figure 5(a), the AgNPs formed without starch and 0.002*M* sodium citrate are assorted in shapes. As the starch concentration is increased to 0.0015*M* [Fig. 5(b)], 0.0029*M* [Fig. 5(c)], and 0.0117*M* [Fig. 5(d)], formation of nearly monodispersed NPs can be observed which can be attributed due to the effective passivation of the surfaces and suppression of the growth of the NPs through strong interactions with the particles via the functional molecular groups of starch. The selected-area ED, Figure 5(e) shows five Debye-Scherrer concentric rings assigned to (111), (200), (220), and (311) planes[57] consistent with the fcc phase of AgNPs and have been confirmed by the XRD results. The particle size histogram of AgNPs shows the distribution of particle sizes ranging from 30 nm to 110 nm, and the average particle size comes out to be 50–90 nm. Further, an increase in the concentration of starch to 0.0117*M*, resulted in the encapsulation of AgNPs in starch polymeric networks as can be seen from Figure 5(d). Usually, the stability of metal NPs is attributed mainly to the adsorption of the polymeric chains onto the crystalline planes of the NPs. The intramolecular and intermolecular

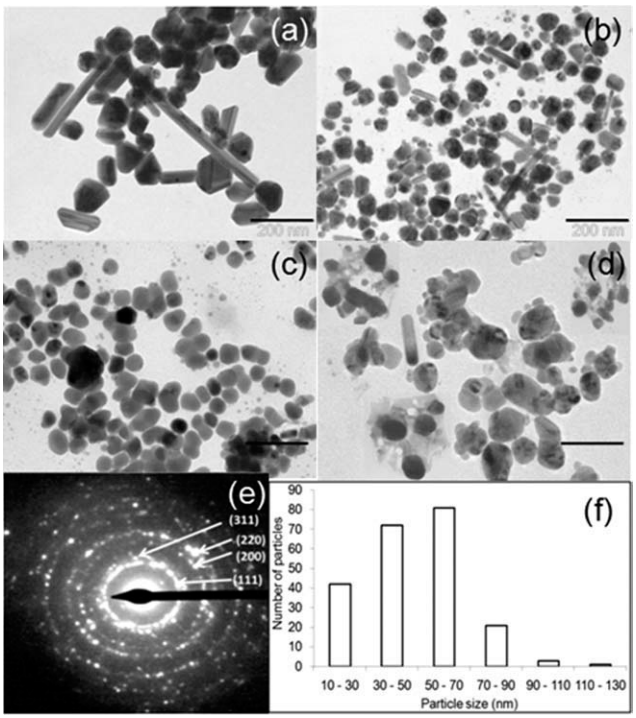

Figure 5 TEM images of silver nanoparticles obtained with increasing concentration of starch (a) with no starch, (b) 0.0015*M*, (c) 0.0029*M*, (d) 0.0117*M*, (e) selected area diffraction, and (f) particle size distribution.

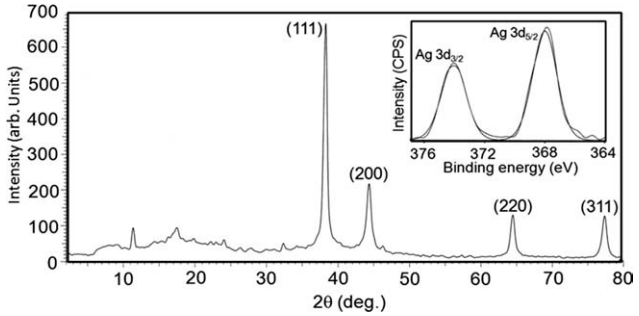

Figure 6 XRD and XPS spectra of silver nanoparticles using both starch and sodium citrate.

association of the starch polymer leads to the formation of hydrogen bonds, which are ultimately responsible for network formation within the polymeric chains, and these networks provide nanoscopic domains in which the NPs can grow like silver–starch core–shell structure.

XRD studies

To know the nature and crystal structure of the AgNPs formed by this approach, XRD and XPS analysis was carried out. The XRD profile presented in Figure 6 exhibits characteristic peaks at scattering angles (2θ) of 38.06, 44.22, 64.48, and 77.32 corresponding to scattering from the (111), (200), (220), and (311) crystallographic planes, respectively. These diffraction peaks firmly represent a face centered cubic structure of crystalline AgNPs.[58]

XPS studies

XPS is an important surface sensitive analytical technique useful for the identification of the surface characteristics of metal NPs. Figure 7 shows the survey scans of pure starch and AgNPs stabilized starch. As can be seen from the survey scans, pure starch shows only two peaks characteristic of C 1s (at 285 eV) and O 1s (at 535 eV), whereas for AgNPs stabilized starch along with C 1s and O 1s peaks, Ag 3d peak at 370 eV is also observed indicating the formation of nanocomposite in which the AgNPs are coated with starch. The high-resolution narrow scan for C 1s for both pure starch and AgNPs stabilized starch are compared in Figure 7(c,d). The deconvolution of C 1s peak indicated three components of carbon. The carbon peak at binding energy 284.6 eV is due to the presence of —C—C— bond and the peaks at 286.2 eV and 287.6 eV are attributed to the presence of —C—O— and —O—C—O—, respectively. The presence of C 1s peaks characteristic of starch in AgNPs, reiterates that the surface of the formed AgNPs is coated with starch leading to the formation of inorganic–organic hybrid material and is in

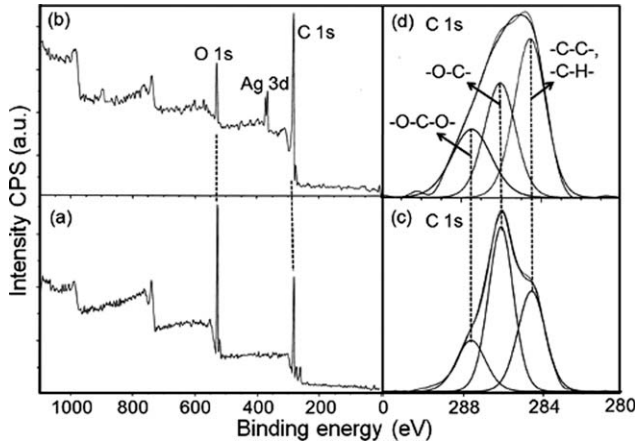

Figure 7 XPS survey scans and high-resolution narrow C 1s scan of (a and c) pure starch and (b and d) silver nanoparticles stabilized starch and sodium citrate, respectively.

consonance with the observations in TGA studies. Moreover, the high-resolution XPS narrow scan of Ag 3d shows a binding energy peak at 368 eV which is deconvoluted into two peaks at the Ag^0 stage ($3d_{5/2}$ and $3d_{3/2}$), which clearly supports the formation of AgNPs[59] (Fig. 6, inset).

Thermal studies

Thermal degradation of polymeric materials is a consequence of the fact that the organic macromolecules inside the polymer matrix as well as low-molecular

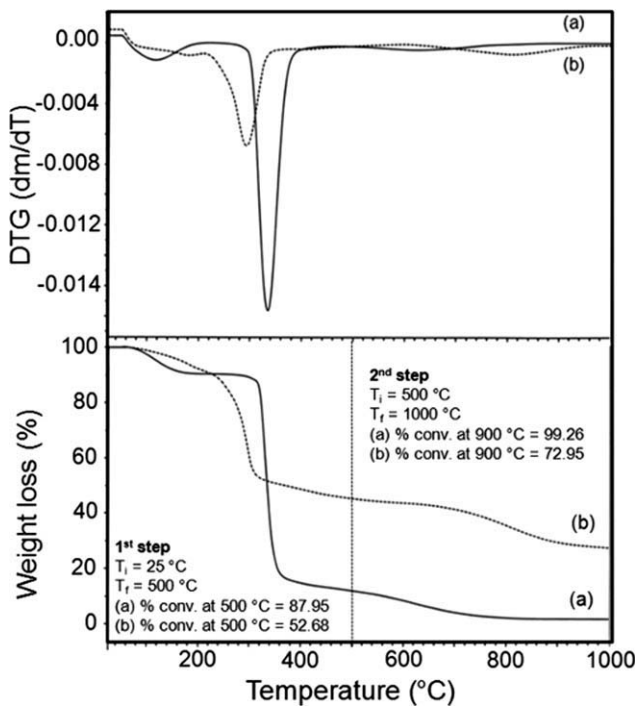

Figure 8 TGA and DTG thermograms (a) pure starch and (b) silver nanoparticles stabilized starch and sodium citrate.

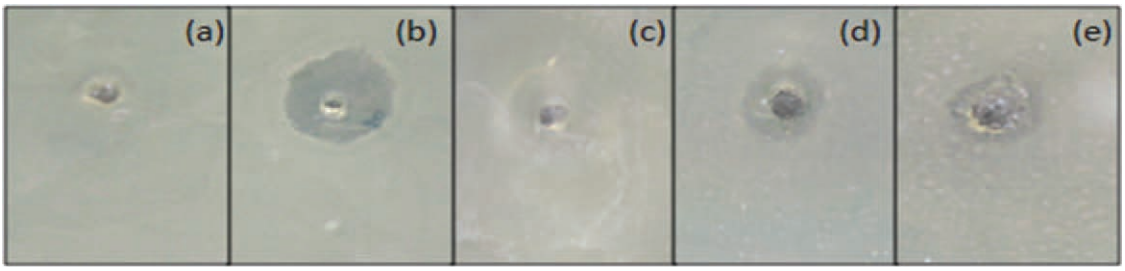

Figure 9 Antimicrobial activity of silver nanoparticles stabilized by (a) starch and Na citrate, antimicrobial activity of silver nanoparticles stabilized by starch alone on (b) *Bacillus subtilis* (c) *Staphylococcus aureus*, (d) *E. coli*, and (e) *Klebsiella* sps. [Color figure can be viewed in the online issue, which is available at wileyonlinelibrary.com.]

weight organic molecules are stable only up to a certain temperature range. Their stability depends on the inherent characteristics of the samples as well as the specific interactions associated between the constituents such as the different macromolecules or molecules, metal NPs, etc. in case of nanocomposites. These interactions are due to the dipole– dipole interaction, van der Waals, London, and hydrogen bonding forces. Figure 8 shows a comparison of the TGA and DTG thermograms of (a) native starch and (b) starch stabilized AgNPs. As can be seen from the figure, both native starch and starch stabilized AgNPs show a similar decomposition profile except that the thermal decompositions are $\sim$ 100% and $\sim$ 70%, respectively, at temperatures greater than 900°C, which clearly suggests that the starch stabilized AgNPs are organic and inorganic hybrid nanocomposites with starch coated on the AgNPs. The decomposition profile shows similar two steps of decomposition for both native starch and starch stabilized AgNPs. In the first step other than the major decomposition of starch in the temperature range 250–400°C, we see loss of adsorbed water in the initial stages of decomposition which is at temperature less than 200°C. At 900°C, as can be seen from Figure 8, the total conversion in the starch stabilized AgNPs is 72.95% when compared with native starch which is about 99.26%, indicates that the remaining 27.05% is the content of Ag metal in the as synthesized sample, i.e., the starch–silver organic–inorganic hybrid nanocomposite.

Antimicrobial activity

The task of this study also includes testing the synthesized AgNPs for the purpose of antibacterial activity. Three samples, i.e., AgNPs synthesized with starch, trisodium citrate, and in combination with both starch and trisodium citrate were taken for the study, and the antibacterial activity was determined against Gram negative organisms by agar diffusion method.[60] The AgNP synthesized using trisodium citrate and in combination with both starch and trisodium citrate did not show any activity against the organisms *Staphylococcus aureus*, *Bacillus subtilis*, *Escherichia coli*, and *Klebsiella* sps as can be seen in Figure 9(a). On the other hand, as can be seen from Figure 9(b–e), AgNP prepared from starch alone were effective against all of these organisms. With 75µl concentration of AgNP, the diameter zone of inhibition observed for *B. subtilis*, *S. aureus*, *E. coli*, and *Klebsiella* sps was 3 mm, 2.4 mm, 1.0 mm, and 1.0 mm, respectively. As the concentration of NPs was increased, the zone of inhibition, which determines the activity of AgNP prepared using starch alone, also increased. Therefore, we conclude that the AgNP synthesized using starch alone shows excellent antibacterial activity.

CONCLUSIONS

We have developed a highly facile, simple method of synthesis of AgNPs showing synergetic effect by using starch and trisodium citrate as reducing and stabilizing agents. The size and shape of the NPs produced can be controlled by varying the concentration of citrate, starch, temperature, pH, and reaction time. Though, pH 7 is the ideal optimum reaction condition, if one wants to eliminate the use of citrate ion, work can be carried out at pH 10. The starch stabilized nanosilver particles were well characterized by UV–Vis, TEM, XRD, XPS, and TGA. AgNP stabilized with starch alone showed good antibacterial activity against *S. aureus*, *B. subtilis*, *E. coli*, and *Klebsiella* sps, whereas AgNP synthesized using trisodium citrate and in combination with both starch and trisodium citrate did not show any activity. The above work can be put into green chemistry perspective, as the choice of the solvent for the synthesis, choice of environmentally benign, nontoxic material for the reduction and stabilization of NPs.

References

1. Hutchinson J. E. ACS Nano 2008, 2, 395.
2. Kamat P. V. J Phys Chem B 2002, 106, 7729.
3. Li I.; Hu J.; Alivistos A. P. Nano Lett 2001, 1, 349.
4. Knoll B.; Keilmann F. Nature 1999, 399, 134.
5. Sengupta S.; Eavarone D.; Capila I.; Zhao G. L.; Watson N.; Kiziltepe T. Nature 2005, 436, 568.

6. Wiley B.; Sun Y.; Xia Y.; Acc Chem Res 2007, 40, 1067.
7. Frattini A.; Pellegri N.; Nicastro D.; de Sanctis O. Mater Chem Phys 2005, 94, 148.
8. Luo C.; Zhang Y.; Wang Y. J Mol Catal A 2005, 229, 7.
9. Lu Y.; Mei Y.; Drechsler M.; Ballauf M. Angew Chem Int Ed 2006, 45, 813.
10. Tao A.; Sinsermsuksaku P.; Yang P. Angew Chem Int Ed 2006, 45, 4597.
11. Wiley B.; Sun Y.; Mayers B.; Xi Y. Chem Eur J 2005, 11, 454.
12. Lisiecki I.; Pileni M. P. J Am Chem Soc 1993, 115, 3887.
13. Yanagihara N.; Tanaka Y.; Okamoto H. Chem Lett 2001, 30, 796.
14. Gaim J.; Fu J.; Lin J.; Han Y.; Yu X.; Pan C. Langmuir 2004, 20, 9775.
15. Kuo P. L.; Chen W. F. J Phys Chem B 2003, 107, 11267.
16. Kim D.; Lee T.; Geckeler K. E. Angew Chem Int Ed 2005, 45, 104.
17. Chen D. H.; Chem Y. Y. Mater Res Bull 2002, 37, 801.
18. Haruta M.; Yamada N.; Geckeler K. E. Angew Chem Int Ed 2005, 45, 104.
19. Qi L.; Gao Y.; Ma J. Colloids Surf A 1999, 157, 285.
20. Behrens S.; Habicht W.; Wagner K.; Unger E. Adv Mater 2006, 18, 284.
21. Naik R. R.; Jones S. E.; Murray C. J.; McAulifee J. C.; Vaia R. A.; Stone M. O. Adv Funct Mater 2004, 14, 25.
22. Crooks R. M.; Zhao M.; Sun L.; Chechik V.; Yeung L. K. Acc Chem Res 2001, 34, 181.
23. Sun X.; Jiang X.; Dong S.; Wang E. Macromol Rapid Commun 2003, 24, 1024.
24. Okugaichi A.; Torigoe K.; Yoshimura T.; Esumi K. Colloids Surf A 2006, 273, 154.
25. Zhao M.; Crooks R. M. Chem Mater 1999, 11, 3379.
26. Zhang J.; Xu S.; Kumacheva E. J Am Chem Soc 2004, 126, 7908.
27. Jin R. H.; Yuan J. J. J Mater Chem 2005, 15, 4513.
28. Geckeler K. E., Ed. Advanced Macromolecular and Supramolecular Materials and Processes; Kluwer Academic/Plenum: NewYork, 2002.
29. Lee P. C.; Meisel D. J Phys Chem 1982, 86, 3391.
30. Shirtcliffe N.; Nickel U.; Schneider S. J Colloid Interface Sci 1999, 211, 122.
31. Nickel U.; Castell A. Z.; Poppl K.; Schneider S. Langmuir 2000, 16, 9087.
32. Chou K. S.; Ren C. Y. Mater Chem Phys 2000, 64, 241.
33. Evanoff D., Jr.; Chumanov G. J. J Phys Chem B 2004, 108, 13948.
34. Sondi I.; Goia D. V.; Matijevic E. J Colloid Interface Sci 2003, 260, 75.
35. Merga G.; Wilson R.; Lynn G.; Milosavljevic B. H.; Meisel D. J Phys Chem C 2007, 111, 12220.
36. Creighton J. A.; Blatchford C. G.; Albrecht M. J. J Chem Soc Faraday Trans 1979, 75, 7902.
37. Ahmadi T. S.; Wang Z. L.; Green T. C.; Henglein A.; El-Sayed M. Science 1996, 272, 1924.
38. Raveendran P.; Jie F.; Wallen S. L. J. Am. Chem. Soc 2003, 125, 13940.
39. Creighton J.; Blatchford C.; Albrecht M. Photochem Photobiol 1994, 60, 605.
40. Schneider S.; Halbig P.; Grau H.; Nickel M. J Chem Soc Faraday Trans 1979, 75, 790.
41. Emory S.; Nie S.; Anal Chem 1997, 69, 2361.
42. Freeman R. G.; Grabar K. C.; Allison K. J.; Bright R. M.; Davis J. A.; Guthrie A. P.; Hommer M. B.; Jackson M. A.; Smith P. C. Science 1995, 267, 1629.
43. Ullman A. Chem Rev 1996, 96, 1533.
44. Zhao M.; Sun L.; Crooks R. M. J Am Chem Soc 1998, 120, 4877.
45. Wang R.; Yang J.; Zheng Z.; Carducci M. D.; Jiao J.; Seraphin S. Angew Chem Int Ed 2001, 40, 549.
46. Zheng J.; Stevenson M. S.; Hikida R. S.; Patten P. G. V. J Phys Chem B 2002, 106, 1252.
47. Frens G.; Nat Phys Sci 1973, 241, 20.
48. Ullman A.; Chem Rev 1996, 96, 1533.
49. Petit C.; Lixon P.; Pileni M.; J Phys Chem B 1993, 97, 129.
50. Suslick K. S.; Fang M.; Hyeon T. J Am Chem Soc 1996, 118, 11960.
51. Ravindran P.; Fu J.; Wallen S. L. Green Chem 2006, 8, 34.
52. Mohan Y. M.; Raju K. M.; Sambasivudu K.; Singh S.; Sreedhar B. J Appl Polym Sci 2007, 106, 3375.
53. (a) Devi D. K.; Pratap S. V.; Haritha R.; Sivudu K. S.; Radhika P.; Sreedhar B. J Appl Polym Sci 2011, 121, 1765. (b) Sreedhar B.; Reddy P. S.; Devi D. K. J Org Chem 2009, 74, 8806. (c) Sreedhar B.; Devi D. K.; Deepthi Y. Catal Commun 2011, 12, 1009.
54. Brown W. H.; Poon T. Introduction to Organic Chemistry, 3rd ed., 2005.
55. Kapoor S.; Lawless D.; Kennepohl P.; Meisel D.; Serpone N. Langmuir 1994, 10, 3018.
56. Mohan Y. M.; Vimala K.; Thomas V. J Colloid Interface Sci 2010, 342, 73.
57. Parashar V.; Parashar R.; Sharma B.; Pandey A. C. Dig J Nanomater Biostruct 2009, 4, 45.
58. (a) Leff D. V.; Brandt L.; Heath J. R. Langmuir 1996, 12, 4723. (b) Swami A.; Kumar A.; Selvakannan P. R.; Mandal S.; Pasricha R.; Sastry M. Chem Mater 2003, 15, 17.
59. Kaushik V. J Electron Spectrosc Relat Phenom 1991, 56, 273.
60. Hewitt W. Microbiological Assay for Pharmaceutical Analysis; CRC Press: UK.